

Riemannian Walk for Incremental Learning: Understanding Forgetting and Intransigence

Arslan Chaudhry*
University of Oxford

arslan.chaudhry@eng.ox.ac.uk

Puneet K. Dokania*
University of Oxford

puneet@robots.ox.ac.uk

Thalaiyasingam Ajanthan*
University of Oxford

ajanthan@robots.ox.ac.uk

Philip H. S. Torr
University of Oxford
philip.torr@eng.ox.ac.uk

Abstract

We study the incremental learning problem for the classification task, a key component in developing life-long learning systems. The main challenges while learning in an incremental manner are to preserve and update the knowledge of the model. In this work, we propose a generalization of Path Integral [24] and EWC [7] with a theoretically grounded KL-divergence based perspective. We show that, to preserve and update the knowledge, regularizing the model's likelihood distribution is more intuitive and provides better insights to the problem. To do so, we use KL-divergence as a measure of distance which is equivalent to computing distance in a Riemannian manifold induced by the Fisher information matrix. Furthermore, to enhance the learning flexibility, the regularization is weighted by a parameter importance score that is calculated along the entire training trajectory. Contrary to forgetting, as the algorithm progresses, the regularized loss makes the network intransigent, resulting in its inability to discriminate new tasks from the old ones. We show that this problem of intransigence can be addressed by storing a small subset of representative samples from previous datasets. In addition, in order to evaluate the performance of an incremental learning algorithm, we introduce two novel metrics to evaluate forgetting and intransigence. Experimental evaluation on incremental version of MNIST and CIFAR-100 classification datasets shows that our approach outperforms existing state-of-the-art baselines in all the evaluation metrics.

1. Introduction

One challenging problem in realizing human-level intelligence is developing systems that can learn new tasks con-

tinually while preserving existing knowledge. Such *continual* or *life-long learning* is difficult to achieve in current AI systems that are built to perform well in one particular task (e.g., classification or segmentation of a *fixed* number of objects), but have minimal flexibility to adapt to new scenarios. In this work, we study a sub-problem of life-long learning, called *incremental learning*.

In a typical offline learning paradigm, once a model is learned for hundreds of tasks, adding a new task requires retraining the model for all the tasks. This would not only require tremendous amount of storage but also a huge training time. In incremental learning, on the other hand, the objective is to train the model just for the new task while preserving existing knowledge. To accomplish this, we focus on developing predictors flexible enough to update their parameters to accommodate new tasks online while still performing well on the previous tasks. While designing such algorithms, we address following problems: (1) *defining knowledge*: how to measure what the model has learned; and (2) *preserving knowledge*: how to learn new tasks while preserving (not forgetting) the previous knowledge.

Knowledge in a neural network can be defined in several ways. A data-based definition, such as *knowledge distillation* [5], assumes that output activations of a network captures the knowledge it had learnt. On the other hand, a model-based approach relies on network parameters to define knowledge. Once the knowledge has been *defined*, the task of preserving and updating the knowledge in an incremental learning set-up has two inherent problems: (1) *catastrophic forgetting*: forgetting existing knowledge; and (2) *intransigence*: updating existing knowledge, such that the network can discriminate current and previous tasks. Both of these problems require tangential solutions and pose a trade-off for any incremental learning algorithm.

Catastrophic forgetting is mainly addressed by regularizing the model. In the case of data-based knowledge, the

*Equal contribution

model is updated such that the new activations do not deviate much from the activations stored using the previous model [14, 21]. This gives flexibility in updating the model parameters while preserving the input-output behaviour. On the other hand, in the case of model-based knowledge, the regularization constrains the new parameters to always be in the vicinity of the old ones [7, 24]. Here, flexibility in learning is achieved through intelligent weighting of the parameters based on their respective importance. In terms of applicability, activation-based regularization might result in huge storage requirements for applications where the activation space itself is very large compared to the network parameters (*e.g.*, semantic segmentation). Keeping this in mind, we focus on the parameters-based regularization. For the other problem of updating the knowledge such that the network not only able to learn new tasks but can also discriminate current and previous tasks, a memory-based set-up is usually required where a small number of representative samples from the previous tasks are stored.

In this work, to counter *catastrophic forgetting*, we learn parameters for the new task such that the model’s likelihood distribution remains in the vicinity of the likelihood distribution obtained using the old parameters. More specifically, along with optimizing the task-specific loss, we also minimize the KL-divergence [9] between the likelihood distributions obtained using the old and the new parameters. To do so, we use the well known second-order approximation of the KL-divergence [2, 19] which allows us to regularize the distributions over the Riemannian manifold induced by the Fisher information matrix. This preserves network’s intrinsic properties while updating for the new tasks. Furthermore, since two different sets of parameters can yield the same output probability distribution, this approach gives more flexibility to the parameters than directly regularizing them in the Euclidean space. In addition, motivated by Path Integral [24], we introduce a *parameter importance score* that is proportional to the sensitivity of the classification loss with respect to the KL-divergence (distance in the Riemannian manifold) between the corresponding output probability distributions. Intuitively, a parameter is weighted higher if it would reduce the loss more for a small movement or walk in the Riemannian manifold. By weighting the KL-divergence with this importance score, the objective incorporates information about both the probability distribution and its influence on the classification loss. By accumulating the score over the optimization trajectory, information about previous tasks is effectively retained. Note that, our method can be seen as a strict generalization of both Elastic Weight Consolidation (EWC) [7] and the Path Integral based method [24] in the Riemannian manifold.

To update the knowledge and counter *intransigence*, we propose different *sampling* strategies to keep a very small subset of the dataset from previous tasks. This would not

only allow the network to *recall* information about the previous tasks but also help in learning to *discriminate* current and previous tasks. Moreover, the literature of continual learning in deep networks lacks the robust metrics to evaluate an incremental learner. For this, we propose two measures to quantify forgetting (very similar to [16]) and intransigence. Experimentally, we set new state-of-the-art results in the incremental versions of MNIST [10] and CIFAR-100 [8], and present extensive analysis to better understand the behaviour of incremental learning algorithms. Our main contributions to the field are:

1. We propose a theoretically grounded KL-perspective that provides novel insights into incremental learning.
2. Our method generalizes recently proposed EWC [7] and path integral [24] methods.
3. We propose evaluation metrics - *Forgetting and Intransigence* - to better understand the behaviour and performance of an incremental learner.
4. We achieve state-of-the-results against different metrics (accuracy, forgetting, and intransigence) on MNIST and CIFAR datasets.

2. Problem Set-up

We focus on the incremental classification task where every new task consists of data with corresponding new labels. Let $\mathcal{D}_k = \{(\mathbf{x}_i^k, y_i^k)\}_{i=1}^{n_k}$ be the dataset corresponding to the k -th task, where $\mathbf{x}_i^k \in \mathcal{X}$ is the input sample and $y_i^k \in \mathcal{Y}^k$ the ground truth label. For example, \mathbf{x}_i^k could be an image and \mathcal{Y}^k a set of labels specific to the k -th task. Under this setting, at the k -th task, the objective is to learn a predictor $f_\theta : \mathcal{X} \rightarrow \mathcal{Y}^k$, where $\theta \in \mathbb{R}^P$ are the parameters of f (a neural network) and $\mathcal{Y}^k = \cup_{j=1}^k \mathcal{Y}^j$. Note that, even though only \mathcal{D}_k is available for the training of k -th task, the output space consists of all the labels seen previously (*single-head*). Were the entire dataset $\cup_{j=1}^k \mathcal{D}_j$ is available for training, the problem would boil down to the standard classification task.

This is in contrast to the standard *multi-head* evaluation criteria of the existing incremental learning algorithms [7, 24] where $\mathcal{Y}^k = \mathcal{Y}^k$. This is a much easier evaluation criteria. For example, let us divide the MNIST dataset into five subsets (for five tasks) as follows: $\{\{0, 1\}, \dots, \{8, 9\}\}$. Then, at the 4-th task, for a given image, the multi-head would predict a class out of two labels $\{6, 7\}$, however, the *single-head* (our) would have to predict a class out of eight classes $\{0, \dots, 7\}$. A much harder evaluation setting as in the case of single-head, the classifier must learn to distinguish labels from different tasks. Note that, single-head is a much more realistic evaluation setting as knowing a priori the subset of labels to look at is a big assumption to make. In extreme situations, where the new task contains

only one label, this would essentially mean knowing a priori the ground truth label itself.

3. Preliminaries

We first briefly review the probabilistic interpretation of neural networks and an approximate form of the KL-divergence both of which are crucial to our approach.

Probabilistic Interpretation of Neural Networks In a probabilistic sense, for a classification task, a neural network models a discrete conditional probability distribution of the form $p_\theta(\mathbf{y}|\mathbf{x})$ (usually the softmax output), where \mathbf{x} is the input and θ are the network parameters (for simplicity, we will use p_θ and $p_\theta(\mathbf{y}|\mathbf{x})$ interchangeably). The prediction label \hat{y} can then be obtained by sampling from a multinoulli distribution, $t(y) = \prod_{j=1}^K p_{\theta,j}^{[y=j]}$, where $p_{\theta,j}$ is the probability of the j -th class, K are the total number of classes in the dataset, and $[\cdot]$ is Iverson bracket. Note that $t(y)$ is defined by p_θ and sampling from it yield a single label/ prediction. Typically, instead of doing such sampling, a label with the highest probability p_θ is chosen as the output of the network.

Approximation of KL-divergence The similarity between any two distributions can be measured using the KL-divergence [9]. Let $D_{KL}(p_\theta \| p_{\theta+\Delta\theta})$ be the KL-divergence between probability distributions defined by the parameters θ and $\theta + \Delta\theta$.

Lemma 3.1. Assuming $\Delta\theta \rightarrow 0$, the second-order Taylor approximation of KL-divergence can be written [2, 19] as:

$$D_{KL}(p_\theta \| p_{\theta+\Delta\theta}) \approx \frac{1}{2} \Delta\theta^\top F_\theta \Delta\theta,^1 \quad (1)$$

where F_θ is the empirical Fisher at θ .

Before explaining the empirical version of a Fisher information matrix, we will first define it in its true form:

Definition 3.1. Fisher Let $p_\theta(\mathbf{y}|\mathbf{x})$ be a probability distribution defined by the parameters θ . The Fisher information matrix at θ can be defined [2] as:

$$\tilde{F}_\theta = \mathbb{E}_{\mathbf{x} \sim \mathcal{D}, \mathbf{y} \sim p_\theta(\mathbf{y}|\mathbf{x})} \left[\left(\frac{\partial \log p_\theta(\mathbf{y}|\mathbf{x})}{\partial \theta} \right) \left(\frac{\partial \log p_\theta(\mathbf{y}|\mathbf{x})}{\partial \theta} \right)^\top \right] \quad (2)$$

where \mathcal{D} is the dataset.

Note that computing this Fisher matrix requires computing gradients using labels sampled from the model distribution $p_\theta(\mathbf{y}|\mathbf{x})$, which requires multiple backward passes (more details are given in the supplementary). Thus, for efficiency, Fisher is often replaced with an empirical Fisher [17], where the expectation is taken over the data distribution, i.e., both \mathbf{x} and \mathbf{y} are now sampled from \mathcal{D} , and we use this to approximate the KL.

¹proof is given in the supplementary material

From the Lemma 3.1, it can be seen that when $\Delta\theta \rightarrow 0$, $D_{KL}(p_\theta \| p_{\theta+\Delta\theta})$ behaves like a distance measure. Therefore, the mapping \mathcal{F} from the parameters $\theta \in \mathbb{R}^P$ to the probability densities p_θ defines a Riemannian manifold², where the Fisher matrix F_θ defines the distance metric. Note that, the distance metric in Riemannian manifold has to be positive definite, but F_θ is positive semi-definite [17]. This makes the manifold quasi-Riemannian.

Note that, the matrix F_θ is of size $P \times P$, which is infeasible to store given the number of parameters in neural networks are normally in the order of millions. Thus, similarly to [7], we assume parameters to be independent of each other which results in the diagonal approximation of F_θ . Thus, Eq. (1) can be written as:

$$D_{KL}(p_\theta \| p_{\theta+\Delta\theta}) \approx \frac{1}{2} \sum_{i=1}^P F_{\theta_i} \Delta\theta_i^2, \quad (3)$$

where θ_i is the i -th entry of the parameter vector θ .

4. Riemannian Walk for Incremental Learning

We will now describe our approach to incremental learning. Briefly, our approach has three key components: (1) KL-divergence based regularization over the conditional probabilities $p_\theta(\mathbf{y}|\mathbf{x})$; (2) parameter importance score based on the sensitivity of loss over the movement in the Riemannian manifold \mathcal{F} ; (3) sampling strategies to handle intransigence. The first two components mitigate the effects of catastrophic forgetting, whereas the third component handles intransigence.

4.1. Avoiding Catastrophic Forgetting

4.1.1 The Objective Function

We first give our objective function and then explain the choice of each component. Given parameters θ^{k-1} trained sequentially from task 1 to task $k-1$, and \mathcal{D}_k for the k -th task, our objective function has the following form:

$$\arg\min_{\theta} \tilde{L}^k(\theta) := L^k(\theta) + \lambda S^{k-1}(\theta) \odot R(\theta, \theta^{k-1}). \quad (4)$$

where $L^k(\cdot)$ is a standard classification loss for task k , $R(\cdot, \cdot)$ is the regularization term, $S^{k-1}(\cdot)$ is parameter importance up to task $k-1$ and λ is a regularization strength which is a hyperparameter. Next we define the regularization term $R(\cdot, \cdot)$. The exact form of the importance $S^{k-1}(\cdot)$ and the operator \odot will be defined later in Section 4.1.4.

4.1.2 KL-divergence-based Regularization

We regularize over the conditional probability distributions $p_\theta(\mathbf{y}|\mathbf{x})$ on the Riemannian manifold \mathcal{F} using

²A Riemannian manifold is a real smooth manifold equipped with an inner product on the tangent space at each point that varies smoothly from point to point [12].

the approximate KL-divergence, Eq. (3), as the distance measure. More precisely, $R(\theta, \theta^{k-1})$ is defined as $D_{KL}(p_{\theta^{k-1}}(\mathbf{y}|\mathbf{x})\|p_{\theta}(\mathbf{y}|\mathbf{x}))$, the KL-divergence between the conditional probability distributions defined by θ^{k-1} and θ , that we want to learn for the new task. Note that in Eq. (3), when θ^{k-1} is at a local minimum, gradients would be nearly zero, making Fisher very small. Hence, the regularization is negligible. To avoid this, similar to [3], we use $F_{\theta^{k-1}} + \eta I$, where $\eta \in \mathbb{R}$ is a hyperparameter and I is the identity matrix. Thus, the KL-based regularization can now be written as:

$$R(\theta, \theta^{k-1}) = \sum_{i=1}^P (F_{\theta_i^{k-1}} + \eta)(\theta_i - \theta_i^{k-1})^2. \quad (5)$$

Note that, when $\eta = 0$, the above regularization is the same as of the EWC [7]. Furthermore, as discussed above, setting η to zero would result in catastrophic forgetting when θ^{k-1} corresponds to a local minimum. This is evidenced in our experiments as EWC ends up forgetting on the first task. However, the use of η would allow us to pass the curvature information which helps to overcome forgetting even when θ^{k-1} is at a local minimum.

Intuitively, the use of KL-divergence would allow the network to learn parameters such that the parametrized distributions of the new and previous tasks are close to each other. This would preserve the inherent properties of the model about previous tasks as the learning progresses.

In what follows we talk about the mathematical form and intuitions behind the parameter importance scores $S^{k-1}(\theta)$ (Eq. (4)), and present our final objective function.

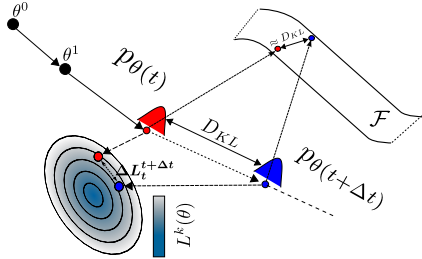


Figure 1: The parameter importance is accumulated over the optimization trajectory where the importance is the sensitivity of improvement in the loss with respect to the KL-divergence which is approximated using the distance in the Riemannian manifold \mathcal{F} .

4.1.3 Optimization Path-based Parameter Importance

In Eq. (5), the Fisher component $(F_{\theta_i^{k-1}} + \eta)$ can be seen as the importance score for the i -th parameter. Since KL-divergence-based parameter importance captures only the intrinsic properties of the model at the minimum, it is

blinded towards the influence of parameters over the entire optimization path. Motivated by [24], we accumulate task-specific parameter importance over the entire training trajectory starting from the first task. Since we are moving in the Riemannian space, the parameter importance is the ratio of the change in loss to the change in distribution induced by the parameters.

More precisely, for a change of parameter from $\theta_i(t)$ to $\theta_i(t + 1)$ (where t is the time step or training iteration), we define parameter importance as the ratio of the change in loss to its influence in $D_{KL}(p_{\theta(t)}\|p_{\theta(t+1)})$. Intuitively, importance will be higher if small change in the distribution causes large improvement over the loss. Formally, using the first-order Taylor series approximation, the loss can be approximated as follows:

$$\begin{aligned} L(\theta(t + \Delta t)) - L(\theta(t)) &\approx - \sum_{i=1}^P \sum_{t=t}^{t+\Delta t} \frac{\partial L}{\partial \theta_i} \Big|_{\theta_i(t)} \delta_i(t), \\ &= - \sum_{i=1}^P \Delta L_t^{t+\Delta t}(\theta_i), \end{aligned} \quad (6)$$

where $\frac{\partial L}{\partial \theta_i} \Big|_{\theta_i(t)}$ is the gradient of the loss w.r.t. θ_i at time step t , $\delta_i(t) = \theta_i(t + 1) - \theta_i(t)$, and $\Delta L_t^{t+\Delta t}(\theta_i)$ represents the accumulated improvement in the loss caused by the change in the parameter θ_i , represented by $\Delta \theta_i(t)$, from time step t to $t + \Delta t$. This $\Delta \theta_i(t)$ would cause change in the model distribution which can be computed using the approximate KL-divergence³ (Eq. (3)). Thus, the importance of the parameter θ_i from training iteration t_1 to t_2 can be computed as:

$$s_{t_1}^{t_2}(\theta_i) = \sum_{t=t_1}^{t_2} \frac{\Delta L_t^{t+\Delta t}(\theta_i)}{F_{\theta_i}^t \Delta \theta_i(t)^2 + \epsilon}, \quad (7)$$

where $\Delta \theta_i(t) = \theta_i(t + \Delta t) - \theta_i(t)$ and $\epsilon > 0$ is to prevent division by zero. The denominator is computed at every discrete intervals of $\Delta t \geq 1$ and $F_{\theta_i}^t$ is computed at every t -th step as described in Section 4.1.5. The computation of this importance score is illustrated in Fig. 1. Since we care about positive influence of parameters, negative scores are set to zero. Note that, in Eq. (7), if the Euclidean distance is used in place of KL divergence, the score will be similar to the one obtained using the path integral approach [24].

4.1.4 Final Objective Function

From Eq. (7), the parameter importance can be computed as $S^{k-1}(\theta_i) = s_{t_0}^{t_{k-1}}(\theta_i)$, where t_0 is the first training iteration and t_{k-1} is the total iterations upto task $k - 1$. Now,

³Note that F_{θ} is used directly to approximate the KL divergence as this computation is done along the path and not at the minimum.

combining Eq. (5), the final objective can be written as:

$$\tilde{L}^k(\theta) = L^k(\theta) + \lambda \sum_{i=1}^P s_{t_0}^{t_{k-1}}(\theta_i)(F_{\theta_i^{k-1}} + \eta)(\theta_i - \theta_i^{k-1})^2. \quad (8)$$

Note that the operation \odot in Eq. (4) becomes a simple scalar multiplication. Furthermore, at any point the additional space complexity is $\mathcal{O}(P)$ as P -dimensional vectors of θ^{k-1} and $F_{\theta^{k-1}}$ are stored. Since our algorithm requires the Fisher matrix for the entire training trajectory (not just at the minimum), efficient computation of Fisher is necessary, which is explained next.

4.1.5 Efficiently Updating Fisher Information Matrix

At a given θ , estimating empirical Fisher F_θ requires us to compute the expectation over the entire dataset, which is expensive. Instead, we use *exponential moving average* to keep on updating the Fisher matrix similar to [18]. Thus, given F_θ^{t-1} at $t-1$, the Fisher is updated as follows:

$$F_\theta^t = \alpha F_\theta^t + (1 - \alpha) F_\theta^{t-1}, \quad (9)$$

where F_θ^t is the Fisher matrix obtained using the current batch and $\alpha \in [0, 1]$ is a hyperparameter. Computing Fisher in this manner contains information about previous tasks, contrary to computing Fisher at the minimum of a task, as done in EWC [7].

4.2. Handling Intransigence

Experimentally we observed that training k -th task with \mathcal{D}_k leads to poor test accuracy for the current task compared to previous tasks. This happens because during training the model has access to \mathcal{D}_k which contains labels \mathbf{y}^k only for the k -th task. However, at test time the label space is over all the tasks seen so far $\mathcal{Y}^k = \cup_{j=1}^k \mathbf{y}^j$, which is much larger than \mathbf{y}^k . This in turn increases the *confusion* at the test time as the predictor function has no means of learning to differentiate the samples of the current task from the ones of previous tasks. An intuitive solution to this problem is to store a subset of representative samples from the previous tasks and use them while training the current task [21]. Below we discuss different strategies to obtain such a subset. Note that we store m points from each task-specific dataset as the training progresses, although it is trivial to have fixed total number of samples for all the tasks, similar to iCaRL [21].

Uniform Sampling A naive yet highly effective (shown experimentally) approach is to sample uniformly random from the previous datasets.

Plane Distance-based Sampling In this case, we assume that samples close to the decision boundary are more representative than the ones far away. For a given sam-

ple $\{\mathbf{x}_i, y_i\}$, we compute the distance⁴ from the decision boundary $d(\mathbf{x}_i) = \phi(\mathbf{x}_i)^\top w^{y_i}$, where $\phi(\cdot)$ is the feature mapping learned by the neural network and w^{y_i} are the last fully connected layer parameters for class y_i . Then, we sample points based on $q(\mathbf{x}_i) \propto \frac{1}{d(\mathbf{x}_i)}$. Here, the intuition is, since we are regularizing over the parameters, the feature space and the decision boundaries do not vary too much. Hence, the samples that lie close to the boundary would act as *boundary defining samples*.

Mean of Features iCaRL [21] proposes a method to find samples based on the feature space $\phi(\cdot)$. For each class y , m number of points are found whose mean in the feature space closely approximate the mean of the entire dataset for that class. However, this subset selection strategy is inefficient compared to both the above sampling methods. In fact, the time complexity is $\mathcal{O}(nfm)$ where n is dataset size, f is the feature dimension and m is the number of required samples.

5. Evaluating Incremental Learners

Incremental learning algorithms are difficult to evaluate as there are not enough proper metrics to understand their behaviour. Towards this, we first give a standard multi-class average accuracy and then propose metrics to evaluate *catastrophic forgetting* and *intransigence*. These metrics capture the trade-off of learning on some tasks are not learning on others.

Average Accuracy (A) Let $a_{k,j} \in [0, 1]$ be the accuracy (fraction of correctly classified images) evaluated on the held-out set of the j -th task ($j \leq k$) after training the network incrementally from task 1 to k . Recall that, the test label space is $\mathcal{Y}^k = \cup_{j=1}^k \mathbf{y}^j$, which contains all the labels seen so far. The average accuracy at task k is defined as:

$$A_k = \frac{1}{k} \sum_{j=1}^k a_{k,j}. \quad (10)$$

This is the multi-class classification accuracy evaluated at task k , which is used in [21]. Note that, the higher the A_k the better the classifier, but this does not provide any information about forgetting or intransigence.

Forgetting Measure (F) To evaluate *catastrophic forgetting*, we define forgetting measure for task j when the model has been incrementally trained from task 1 to k as:

$$f_j^k = \max_{l \in \{1, \dots, k-1\}} a_{l,j} - a_{k,j}, \quad \forall j < k. \quad (11)$$

Note that, $f_j^k \in [-1, 1]$ is defined for $j < k$ as we are interested in measuring how much the learner has forgotten about *previous* tasks. To normalize against the number

⁴In fact, d is proportional to the distance from decision boundary w^{y_i} .

of tasks seen previously, the average forgetting at k -th task would then be:

$$F_k = \frac{1}{k-1} \sum_{j=1}^{k-1} f_j^k. \quad (12)$$

If $\max_{l \in \{1, \dots, k-1\}} a_{l,j}$ is replaced with $a_{j,j}$, then F_k has the same form as the negative of Backward Transfer (BWT) [16], but F_k is more generic than BWT as it captures the effect of *positive transfer learning* (PTL) - when learning new tasks improve the accuracy of a previous task. Lower F_k implies less forgetting on previous tasks after training the model for the k -th task. $f_j^k < 0$, implies PTL on task j after training for task k .

Intransigence Measure (I) As explained in Section 4.2, intransigence is the *inability* of an incremental learner to update its knowledge about the current task. This is mainly caused by the unavailability of the data from the previous tasks which in turn does not allow the algorithm to learn to differentiate among current and previous tasks. To quantify this, we train a new reference model with complete datasets of all the tasks from 1 to k combined ($\bigcup_{l=1}^k \mathcal{D}_l$) and measure its accuracy on the held-out set of k -th task, denoted as a_k^* . We then define the intransigence measure for the task k as:

$$I_k = a_k^* - a_{k,k}, \quad (13)$$

where $a_{k,k}$ denotes the accuracy on the k -th task for a model trained *incrementally* from tasks 1 to k . Note that $I_k \in [-1, 1]$ and $I_k < 0$ implies learning incrementally for task k is better than learning from the combined datasets of all the tasks from 1 to k . Lower the value of I_k the better the method is at learning new tasks.

6. Related Work

One way to address catastrophic forgetting is by dynamically expanding the network for each new task [11, 20, 22, 23]. Though intuitive and simple, these approaches are not scalable as the size of the network increases with the number of tasks. A better strategy would be to exploit the overparametrization of neural networks [4]. This entails regularizing either over the activations (output) [14, 21] or over the network parameters [7, 24]. Even though activation-based approach allows more flexibility in parameter updates, it is memory inefficient if the activations are in millions, *e.g.* semantic segmentation. On the contrary, methods that regularize over the parameters - weighting the parameters based on their individual *importance* - are suitable for such tasks. Our method falls under the latter category and we show that our method is a strict generalization of both EWC [7] and the path integral-based method [24]. Different from the above approaches, Lopez-Paz *et al.* [16] update gradients based on the gradients from the previous tasks, while Lee *et al.* [13] uses moment matching to obtain network weights as the combination of the weights of all the tasks.

7. Experimental Results and Analysis

In Section 7.1, we give an overview of the experimental set-up including baselines and datasets. Sections 7.2 and 7.3 provide extensive comparison of our method with the baselines using measures defined in Section 5 and provides in-depth analysis to understand *forgetting* and *intransigence*.

We achieve improvements of 13.8% and 10.0% over the best baseline (in their original form) in average accuracy for MNIST and CIFAR, respectively, while at the same time maintaining very low forgetting and intransigence. However, for fair comparisons, we slightly modify the baselines (PI [24] and EWC [7]) to allow them to incorporate samples from the previous tasks, thus, making them as strong as possible. This, as expected, reduces our improvement to 4.7% and 1.3% in terms of average accuracy for MNIST and CIFAR, respectively. However, in terms of forgetting and intransigence, as will be discussed, our algorithm provides a much better trade-off.

7.1. Experimental Set-up, Baselines and Datasets

Experimental Set-up As mentioned earlier, when training for the task k only \mathcal{D}_k is available, unless otherwise specified. Furthermore, during evaluation, the classification accuracy $a_{k,j}$ on task j after training for k tasks is evaluated for all $j \in \{1 \dots k\}$. The task based loss (L^k in Eq. (4)) is set to softmax cross-entropy and Adam optimizer [6] (learning rate = 1×10^{-3} , $\beta_1 = 0.9$, $\beta_2 = 0.999$) is used with batch size 64. All hyperparameters in Eq. (4) and baselines are found using grid search and the best values for each dataset are given in the supplementary material. The parameters at the start of the algorithm are randomly initialized with Gaussian (0, 0.1) and subsequent tasks are initialized with the weights from the previous task.

Baselines We first compare our method against a standard unregularized network (Vanilla) and two state-of-the-art methods: Elastic Weight Consolidation (EWC) [7] and Path Integral (PI) [24], where we do not use samples in any method. Then, we evaluate the effect of storing a small subset of samples (obtained by *uniform sampling*, other subset selection strategies are discussed in Section 7.3) for each task and compare our method with EWC and PI with sampling. While sampling, class imbalance is handled by weighting the corresponding loss with inverse class frequency similar to [15]. During sampling experiments, we also compare against iCaRL [21], an algorithm based on knowledge distillation [5] and specifically designed to handle incremental classification. We tested both the versions of iCaRL: *hybrid1* (denoted as iCaRL-hb1) that uses network output for classification and the other based on mean-of-exemplar classifier (denoted as iCaRL). Except iCaRL (where the authors' implementation is used) all the other methods are implemented in Tensorflow [1].

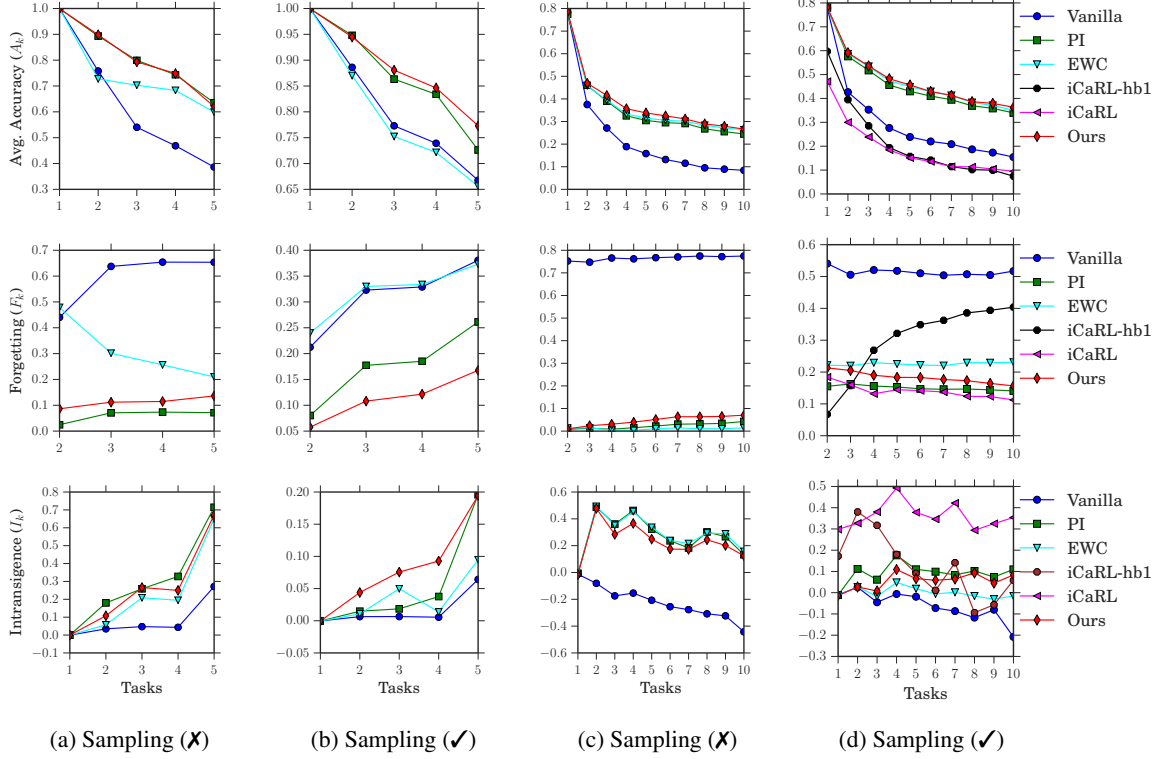


Figure 2: **MNIST (left two) and CIFAR (right two) results with and without sampling.** Our method performs comparable to second best (PI) in MNIST without sampling and outperforms all the other baselines in remaining settings. Note that, on MNIST without sampling EWC forgets on the first task which can be explained by a vanishing Fisher at the local minimum, see Section 4.1.2. (best viewed in color)

Incremental MNIST The MNIST dataset is split into 5 disjoint subsets where each subset corresponds to two consecutive classes, *i.e.*, $\cup_k \mathbf{y}^k = \{\{0, 1\}, \dots, \{8, 9\}\}$. For this setting, similar to [24], a network with two hidden layers, each with 256 units and ReLU nonlinearities is used. While sampling, only 10 samples per class (0.2%) are stored.

Incremental CIFAR-100 Similarly, CIFAR-100 dataset is split into 10 disjoint subsets such that $\cup_k \mathbf{y}^k = \{\{0 - 9\}, \dots, \{90 - 99\}\}$. A convolutional network (4 convolutional, followed by 1 dense layer with dropout and ReLU) is used (exhaustive details of the network are provided in the supplementary). While sampling, only 25 samples per class (5%) are stored. Note that, for iCaRL, the network used in this paper is smaller than the one used in the original paper. The purpose of our evaluation is to show the performance of all the methods for a given architecture.

7.2. Results

We compare different methods in terms of accuracy A_K , forgetting F_K , and intransigence I_K (explained in Section 5). A comparison is shown in Table 1 and different plots are provided in Fig. 2. As evident, our method with sampling performs better than all the other methods (with

and without sampling) in both MNIST and CIFAR in terms of accuracy, a standard metric used by all the state-of-the-art methods [21]. However, the strength of our algorithm also lies in its ability to strike a balance between forgetting and intransigence, which further consolidates the effectiveness of our approach.

7.3. Understanding Forgetting and Intransigence

In this section, we answer several questions in order to better understand the trade-off between forgetting and intransigence which eventually will help us in choosing a reliable incremental learner. We also discuss the effect of sampling on all the evaluation metrics.

Trade-off between Forgetting and Intransigence To better evaluate an incremental learning algorithm, we must analyse its behaviour in terms of forgetting and intransigence. We provide Fig. 3 for better understanding. A good incremental learner need to be at the bottom left corner of the plot. As shown in the figure, our method, even if not lowest in both the measures, achieves a better trade-off compared to the baselines.

	MNIST			CIFAR-100		
	A_5 (%)	F_5	I_5	A_{10} (%)	F_{10}	I_{10}
Vanilla	38.6	0.65	0.27	8.4	0.77	-0.44
EWC	59.8	0.21	0.65	26.3	0.02	0.16
PI	63.5	0.07	0.71	24.4	0.04	0.13
Ours	62.1	0.13	0.67	27.1	0.07	0.12
Vanilla-S	66.7	0.38	0.06	15.4	0.52	-0.21
PI-S	72.6	0.26	0.20	33.9	0.14	0.11
EWC-S	65.6	0.37	0.10	35.0	0.23	-0.02
iCaRL-hb1	36.6	0.68	-0.002	7.4	0.40	0.06
iCaRL	55.8	0.19	0.46	9.5	0.11	0.35
Ours-S	77.3	0.16	0.19	36.3	0.15	0.08

Table 1: Comparison with baselines on average accuracy A_K , forgetting F_K and intransigence I_K measures after the sequential training on MNIST ($K = 5$) and CIFAR-100 ($K = 10$) datasets. When a subset of previous samples are stored (sampling), the method name is appended with ‘-S’. iCaRL-hb1 and iCaRL by default uses subset of previous task datasets. Note that, only 0.2% and 5% of the previous samples are stored for MNIST and CIFAR, respectively. A method is good if it has high value of A_K and, low values of F_K and I_K . The main purpose of F_K and I_K is to understand the behaviour of different algorithms.

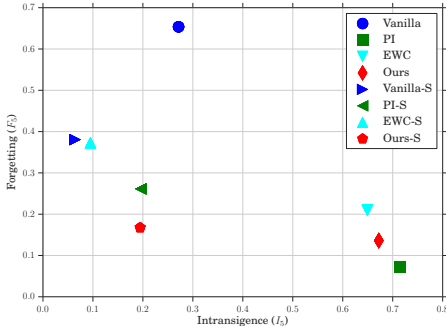


Figure 3: Comparison of different methods against both the forgetting and intransigence on MNIST. The closer the algorithm is to the origin the better it is. Our method finds a suitable compromise between forgetting and intransigence thereby lying closest to the origin. (best viewed in color)

Effects of Sampling on Evaluation Metrics Let us look back into the Table 1. Recall that only 0.2% and 5% samples were stored for MNIST and CIFAR datasets, respectively. It is evident from the table that storing previous task samples significantly improves the accuracy and intransigence measures. However, as can be seen, it has a slight adverse effect on the forgetting measure. The same can be observed from the plots in Fig. 2. Here, we shed some light as to why this would happen. We pick PI and Our method to understand the effects of sampling on MNIST. Storing

previous samples improved accuracy of PI and Our method by 9.1% and 15.2%, respectively. Similarly, with sampling, intransigence improves by 0.51 and 0.48 points on PI and Our method, respectively.

Why storing small number of previous samples makes Forgetting worse? From Table 1 and Fig. 2 we can see that forgetting gets worse if *small* number of samples from previous tasks are used. We argue that this is because when we use samples, we have to train the discriminant weights of the previous tasks in the last layer of the network. Given the small size of the representative samples from the previous tasks, despite the regularization loss, the network ends up changing these parameters in a suboptimal way. Note that, an algorithm with better regularization would be less susceptible to this behaviour. From Table 1 we could see that on PI forgetting gets worse by 19% when small number of previous samples are used, whereas our method suffers by only 3%. This confirms that the regularization employed in our method is more effective than PI. However, as we will show in the supplementary material forgetting eventually improves if the number of samples are increased beyond a certain threshold.

Why negative intransigence for Vanilla? In Table 1 and Fig. 2 we see that intransigence measure goes to negative values for Vanilla and EWC-S in CIFAR-100. This could potentially happen because of the simplicity of the current task. Recall that in Eq. (13) a_k^* is evaluated after training the network for $\bigcup_{l=1}^k \mathcal{D}_l$, whereas $a_{k,k}$ is evaluated after training just with \mathcal{D}_k and a small subset from $\bigcup_{l=1}^k \mathcal{D}_l$ (in case of sampling). In the later case, the network can easily overfit to the current class labels and give better performance on the current task than training with all the tasks together, thereby giving negative intransigence.

Why iCaRL is performing so poor? For iCaRL, the average accuracy (A_{10}) reported in the original paper [21] is $\approx 50\%$. However, in our experimental setting the performance of iCaRL is worse than vanilla. The only difference between the two settings is the network architecture where the original paper used ResNet-32, we used a less expressive 4-layer CNN. Since the regularization of iCaRL is based on the network output and the classifier is based on mean-of-exemplars, that depends on the feature space, less expressiveness of the network might have resulted in poor performance. On the other hand, since we directly regularize over the parameters, our network is less sensitive to the network architecture.

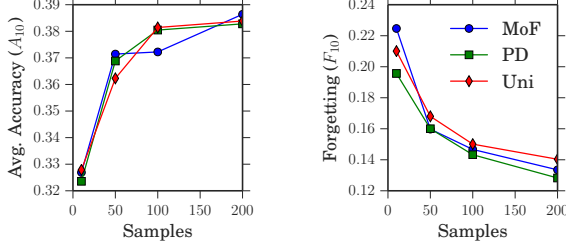


Figure 4: Comparison of subset selection strategies with our method in CIFAR. All the strategies perform similar while PD is slightly better on forgetting measure. (best viewed in color)

7.4. Different Sampling Strategies

In Fig. 4 we compare Mean-of-Features (MoF), Plane-Distance (PD) and Uniform Sampling (Uni) strategies, discussed in Section 4.2, against the number of samples on CIFAR-100. We observe that, despite being computationally expensive, MoF does not perform particularly well over the other strategies. PD-based sampling is the best performing in the forgetting measure, *i.e.*, finding samples that lie close to the boundary helps the network to retain the previous knowledge. While being naive, uniform sampling is highly effective as it finds diverse samples.

8. Discussion

In this work, we have critically analyzed the challenges in an incremental learning problem, namely, catastrophic forgetting and intransigence. To tackle catastrophic forgetting, we have presented an incremental learning algorithm that regularizes the KL-divergence between the conditional probability distributions defined by the parameters of the neural network. In addition to that, to enhance flexibility in learning, a parameter importance, based on sensitivity of the loss with respect to the change in KL, is introduced. In addition to that, not-learning is handled using sampling strategies based on feature space and decision boundaries. Our complete algorithm is memory efficient compared to knowledge distillation based algorithms such as iCaRL [21], which would enable the possibility of incremental learning on segmentation tasks. Furthermore, we have introduced metrics to measure forgetting and intransigence, which we believe, would be useful to better evaluate incremental learning algorithms.

Acknowledgements

This work was supported by The Rhodes Trust, EP-SRC, ERC grant ERC-2012-AdG 321162-HELIOS, EP-SRC grant Seebibyte EP/M013774/1 and EPSRC/MURI grant EP/N019474/1.

Supplementary Material

For the sake of completeness we first give more details on the KL divergence approximation using Fisher information matrix (Section 3). In particular, we give the proof of Lemma 3.1, discuss the difference between the true Fisher and the empirical Fisher⁵ and explain why the Fisher goes to zero at a minimum. Later, in Section B we provide the details of the network architecture and additional experimental results are given in Section C.

A. Approximate KL divergence using Fisher Information Matrix

A.1. Proof of Lemma 2.1

Lemma A.1. Assuming $\Delta\theta \rightarrow 0$, the second-order Taylor approximation of KL-divergence can be written [2, 19] as:

$$D_{KL}(p_\theta \| p_{\theta+\Delta\theta}) \approx \frac{1}{2} \Delta\theta^\top \tilde{F}_\theta \Delta\theta, \quad (14)$$

where F_θ is the empirical Fisher at θ .

The proof is similar to the one presented in [19].

Proof. The KL divergence can be expanded as:

$$D_{KL}(p_\theta(\mathbf{z}) \| p_{\theta+\Delta\theta}(\mathbf{z})) = \mathbb{E}_{\mathbf{z}} [\log p_\theta(\mathbf{z}) - \log p_{\theta+\Delta\theta}(\mathbf{z})]. \quad (15)$$

Note that we use the shorthands $p_\theta(\mathbf{z}) = p_\theta(\mathbf{y}|\mathbf{x})$ and $\mathbb{E}_{\mathbf{z}}[\cdot] = \mathbb{E}_{\mathbf{x} \sim \mathcal{D}, \mathbf{y} \sim p_\theta(\mathbf{y}|\mathbf{x})}[\cdot]$. We denote partial derivatives as column vectors. Let us first write the second order Taylor series expansion of $\log p_{\theta+\Delta\theta}(\mathbf{z})$ at θ :

$$\log p_{\theta+\Delta\theta} \approx \log p_\theta + \Delta\theta^\top \frac{\partial \log p_\theta}{\partial \theta} + \frac{1}{2} \Delta\theta^\top \frac{\partial^2 \log p_\theta}{\partial \theta^2} \Delta\theta. \quad (16)$$

Now, by substituting this in Eq. (15), the KL divergence can be written as:

$$D_{KL}(p_\theta \| p_{\theta+\Delta\theta}) \approx \mathbb{E}_{\mathbf{z}} [\log p_\theta] - \mathbb{E}_{\mathbf{z}} [\log p_{\theta+\Delta\theta}] \quad (17a)$$

$$\begin{aligned} & - \Delta\theta^\top \mathbb{E}_{\mathbf{z}} \left[\frac{\partial \log p_\theta}{\partial \theta} \right] - \frac{1}{2} \Delta\theta^\top \mathbb{E}_{\mathbf{z}} \left[\frac{\partial^2 \log p_\theta}{\partial \theta^2} \right] \Delta\theta, \\ & = \frac{1}{2} \Delta\theta^\top \mathbb{E}_{\mathbf{z}} \left[- \frac{\partial^2 \log p_\theta}{\partial \theta^2} \right] \Delta\theta \quad \text{see Eq. (18)}, \\ & = \frac{1}{2} \Delta\theta^\top \bar{H} \Delta\theta \quad \text{see Eq. (19b)}. \end{aligned} \quad (17b)$$

In Eq. (17a), if the expectation is taken such that, $\mathbf{x} \sim \mathcal{D}, \mathbf{y} \sim p_\theta(\mathbf{y}|\mathbf{x})$, the first order partial derivatives cancels

⁵By Fisher, we always mean the empirical Fisher.

out, *i.e.*,

$$\begin{aligned}
\mathbb{E}_{\mathbf{z}} \left[\frac{\partial \log p_{\theta}(\mathbf{z})}{\partial \theta} \right] &= \mathbb{E}_{\mathbf{x} \sim \mathcal{D}} \left[\sum_{\mathbf{y}} p_{\theta}(\mathbf{y}|\mathbf{x}) \frac{\partial \log p_{\theta}(\mathbf{y}|\mathbf{x})}{\partial \theta} \right], \\
&= \mathbb{E}_{\mathbf{x} \sim \mathcal{D}} \left[\sum_{\mathbf{y}} p_{\theta}(\mathbf{y}|\mathbf{x}) \frac{1}{p_{\theta}(\mathbf{y}|\mathbf{x})} \frac{\partial p_{\theta}(\mathbf{y}|\mathbf{x})}{\partial \theta} \right], \\
&= \mathbb{E}_{\mathbf{x} \sim \mathcal{D}} \left[\frac{\partial}{\partial \theta} \sum_{\mathbf{y}} p_{\theta}(\mathbf{y}|\mathbf{x}) \right], \\
&= \mathbb{E}_{\mathbf{x} \sim \mathcal{D}} [0] = 0.
\end{aligned} \tag{18}$$

Note that this holds for the continuous case as well, where assuming sufficient smoothness and the fact that limits of integration are constants (0 to 1), the Leibniz's rule would allow us to interchange the differentiation and integration operators.

Additionally, in Eq. (17b), the expected value of negative of the Hessian can be shown to be equal to the true Fisher matrix (\tilde{F}) by using Information Matrix Equality.

$$\mathbb{E}_{\mathbf{z}} \left[-\frac{\partial^2 \log p_{\theta}(\mathbf{z})}{\partial \theta^2} \right] = -\mathbb{E}_{\mathbf{z}} \left[\frac{1}{p_{\theta}(\mathbf{z})} \frac{\partial^2 p_{\theta}(\mathbf{z})}{\partial \theta^2} \right] \tag{19a}$$

$$\begin{aligned}
&+ \mathbb{E}_{\mathbf{z}} \left[\left(\frac{\partial \log p_{\theta}(\mathbf{z})}{\partial \theta} \right) \left(\frac{\partial \log p_{\theta}(\mathbf{z})}{\partial \theta} \right)^{\top} \right], \\
&= -\mathbb{E}_{\mathbf{z}} \left[\frac{1}{p_{\theta}(\mathbf{z})} \frac{\partial^2 p_{\theta}(\mathbf{z})}{\partial \theta^2} \right] + \tilde{F}_{\theta}
\end{aligned} \tag{19b}$$

- If in Eq. (19b), the expectation is taken such that, $\mathbf{x} \sim \mathcal{D}$, $\mathbf{y} \sim p_{\theta}(\mathbf{y}|\mathbf{x})$, the first term cancels out by following a similar argument as in Eq. (18). Hence, the expected value of negative of the Hessian equals true Fisher matrix.
- However, if in Eq. (19b), the expectation is taken such that, $(\mathbf{x}, \mathbf{y}) \sim \mathcal{D}$, the first term does not go to zero, and \tilde{F}_{θ} becomes the *empirical Fisher matrix* (F_{θ}).
- Additionally, at the optimum, since the model distribution approaches the true data distribution, hence even sampling from dataset *i.e.*, $(\mathbf{x}, \mathbf{y}) \sim \mathcal{D}$ will make the first term to approach zero, and $\tilde{H} \approx F_{\theta}$.

With the approximation that $\tilde{H} \approx \tilde{F}_{\theta} \approx F_{\theta}$, the proof of the lemma is complete. \square

Note that, as we will argue in Section A.2.2 the true Fisher matrix is expensive to compute as it requires multiple backward passes, instead, we use empirical Fisher to approximate the KL-divergence.

A.2. Empirical and True Fisher at a Local Minimum

Let ' q ' be any reference distribution and ' p ' (parametrized by θ) be the model distribution obtained after applying softmax on the class scores, denoted by s . The cross-entropy loss between q and p can be written as: $\ell(\theta) = -\sum_j q_j \log p_j$. The gradients of the loss with respect to the class scores are:

$$\frac{\partial \ell(\theta)}{\partial s_j} = p_j - q_j. \tag{20}$$

By chain rule, the gradients with respect to the model parameters are $\frac{\partial \ell(\theta)}{\partial \theta} = \frac{\partial \ell(\theta)}{\partial \mathbf{s}} \frac{\partial \mathbf{s}}{\partial \theta}$.

A.2.1 Empirical Fisher

In case of an empirical Fisher, since the expectation is taken such that $(\mathbf{x}, \mathbf{y}) \sim \mathcal{D}$, the ' q ' becomes a Dirac delta distribution (δ). Then, Eq. (20) becomes:

$$\frac{\partial \ell(\theta)}{\partial s_j} = \begin{cases} p_j - 1, & \text{if 'j' is the ground truth label,} \\ p_j, & \text{otherwise.} \end{cases}$$

Now, if at the minimum $p \rightarrow q$ and, since ' q ' is a delta distribution, the gradients $\frac{\partial \ell(\theta)}{\partial s_j} \rightarrow 0$. Consequently, by chain rule $\frac{\partial \ell(\theta)}{\partial \theta} \rightarrow 0$. On the other hand, even if p does not approach q , since we are at a local minimum the gradients $\frac{\partial \ell(\theta)}{\partial \theta} \rightarrow 0$. Since the Fisher is the expectation of the product of gradients $\left(\frac{\partial \ell(\theta)}{\partial \theta} \right)$, it also approaches to zero.

A.2.2 True Fisher

In case of true Fisher, since the expectation is taken such that $\mathbf{x} \sim \mathcal{D}$, $\mathbf{y} \sim p_{\theta}(\mathbf{y}|\mathbf{x})$, the ' q ' becomes a categorical distribution sampled from a multinoulli distribution defined by ' p ', (*i.e.*) $q \sim t(y)$, where $t(y) = \prod_{j=1}^K p_j^{[y=j]}$, where $[.]$ is Iverson bracket. The gradients in Eq. (20) now depend on the sampling from the multinoulli ' t '. At the minimum, since the model distribution ' p ' becomes peaky around the ground truth label, the ' t ' closely mimics a delta distribution at the ground truth label index. Sampling ' q ' from this delta distribution would, again, make the gradients in Eq. (20) close to zero. Consequently, the true Fisher would also approach to zero. However, due to sampling, albeit from a peaky distribution, true Fisher is less susceptible to approaching zero at the minimum than the empirical Fisher. However, in order to compute the expectation, since ' q ' has to be sampled multiple times from ' t ', the true Fisher requires multiple backward passes. This makes it prohibitively expensive to compute and we resort to the empirical Fisher approximation instead.

B. Model Architecture and Hyperparameters

B.1. Architecture

In Table 2 we report the detailed architecture of the convolutional network used in the incremental CIFAR-100 experiments (Section 7.1). Note that, in comparison to [24], we use only one fully-connected layer (denoted as ‘FC’ in the table). For each task k , the weights in the last layer of the network can be dynamically added.

Table 2: *Convolutional network architecture for incremental CIFAR-100. Here, ‘n’ denotes the number of classes in each task.*

Operation	Kernel	Stride	Filters	Dropout	Nonlin.
3x32x32 input					
Conv	3×3	1×1	32		ReLU
Conv	3×3	1×1	32		ReLU
MaxPool		2×2		0.5	
Conv	3×3	1×1	64		ReLU
Conv	3×3	1×1	64		ReLU
MaxPool		2×2		0.5	
Task 1: FC			n		
... : FC			n		
Task k: FC			n		

B.2. Hyperparameters

In Table 3 we report the best hyperparameters for each method, namely, EWC [7], PI [24] and our method used in all the experimental settings reported in the Sections 7.1 and 7.2 and in the next section, unless otherwise specified.

C. Additional Experiments and Analysis

In this section, we first do an ablation study to highlight the importance of each components of our algorithm. Then, we provide more detailed analysis of all the methods.

C.1. Ablation Analysis

In Table 4 we provide average accuracy (A_K), forgetting measure (F_K) and intransigence measure (I_K) (see Section 5) by incrementally adding different components of our method in both MNIST and CIFAR-100 datasets. In particular, we show the merits of adding ηI to Fisher, which improves the forgetting measure, and then incorporating parameter importance scores on top of that, which improves intransigence by allowing flexibility in learning. Note that we used the best hyperparameters settings of our method reported in Table 3 to run the ablation experiments. Additionally, we can, again, see the interplay of *Forgetting* and *Intransigence* measures in the first and the last row of the table.

Table 3: *Best settings for model hyperparameters for different methods on MNIST and CIFAR datasets. Here, λ sets the trade-off between task loss and regularization, η captures the constant curvature, α used in exponential moving average computation of Fisher and Δt is the interval used to accumulate parameter importance (see Eq. (7) (8) and (9)).*

Dataset/ Arch.	Method	Sampling	λ	η	α	Δt
MNIST/ MLP	PI	\times	0.1	-	-	-
		\checkmark	0.1	-	-	-
	EWC	\times	75×10^3	-	-	-
		\checkmark	75×10^3	-	-	-
	Ours	\times	10	0.001	0.1	100
		\checkmark	1	10	0.5	1
CIFAR-100/ Conv. Net.	PI	\times	0.1	-	-	-
		\checkmark	10	-	-	-
	EWC	\times	75×10^3	-	-	-
		\checkmark	75×10^5	-	-	-
	Ours	\times	10	0.01	0.1	500
		\checkmark	1	0.1	0.9	50

Table 4: *Incremental MNIST and CIFAR-100 without sampling: How different performance metrics vary as we add different components of our proposed model (Eq. (8)). Best hyperparameter settings from Table 3 are used.*

Dataset	Setting	A_K (%)	F_K	I_K
MNIST	F	38.4	0.66	0.21
	$(F + \eta I)$	47.9	0.08	0.71
	Full ($S(F + \eta I)$)	62.1	0.13	0.67
CIFAR-100	F	11.7	0.62	-0.37
	$(F + \eta I)$	9.1	0.008	0.37
	Full ($S(F + \eta I)$)	27.1	0.07	0.12

C.2. Task-Level Analysis

In Figs. 5 and 7, we compare the accuracy of different tasks on MNIST and CIFAR-100, respectively, as the model is trained for new classes. The plots show that, without sampling, *Vanilla* setting ends up learning better for the current task as it does not regularize over the weights of previous tasks. This results in a very small *Intransigence Measure*. On the other hand, this setting results in *catastrophic forgetting* as shown in the plots. Similarly to CIFAR, the performance of iCaRL is worse than our method. In short, the conclusion of the main paper holds.

Furthermore, note the forgetting on the first task when EWC is used to compute the parameter importance in the first row of Fig. 5. This happens because, as argued in Section 4.1.2, for the first task, due to simple unregularized loss, the model finds a θ^1 that corresponds to a local minimum. This makes the empirical Fisher (F_{θ^1}) close to zero. In our formulation (as discussed in Section 4.1.2) non-

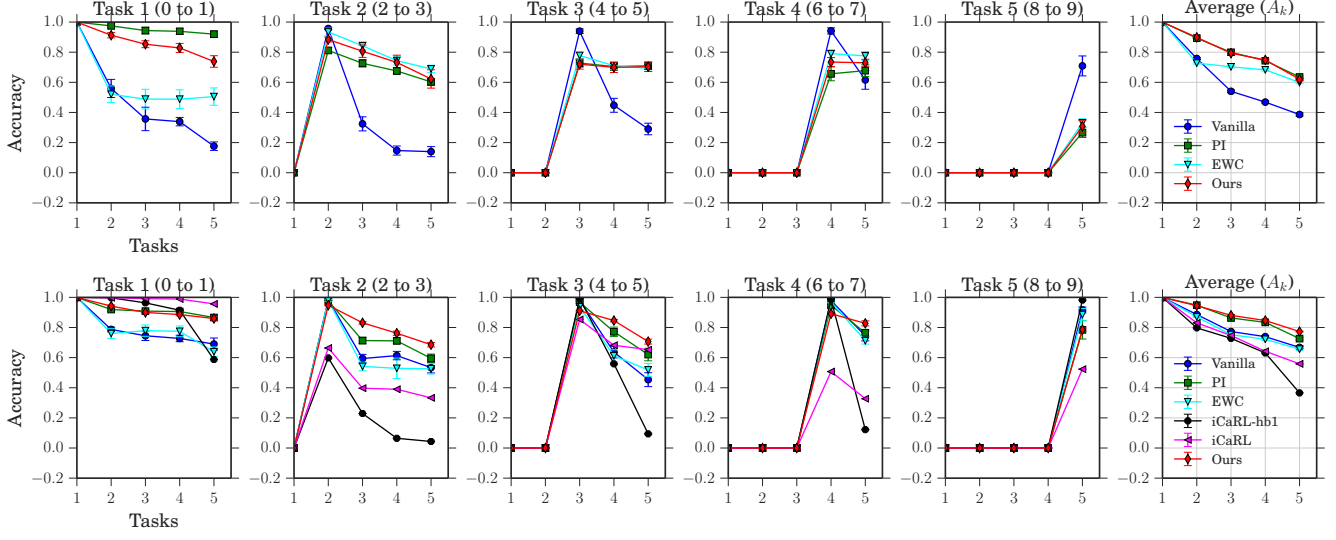


Figure 5: Accuracy measure in incremental MNIST without (**top**) and with (**bottom**) sampling. The first five plots show how the performance of different tasks vary as the model is trained for new tasks e.g. the first plot depicts the variation in performance on Task 1 when the network is sequentially trained for the five tasks in an incremental manner. The last plot is the average accuracy measure as defined in Eq. (10). Note: iCaRL plots for MNIST (not in the original iCaRL paper) are also shown. (best viewed in color)

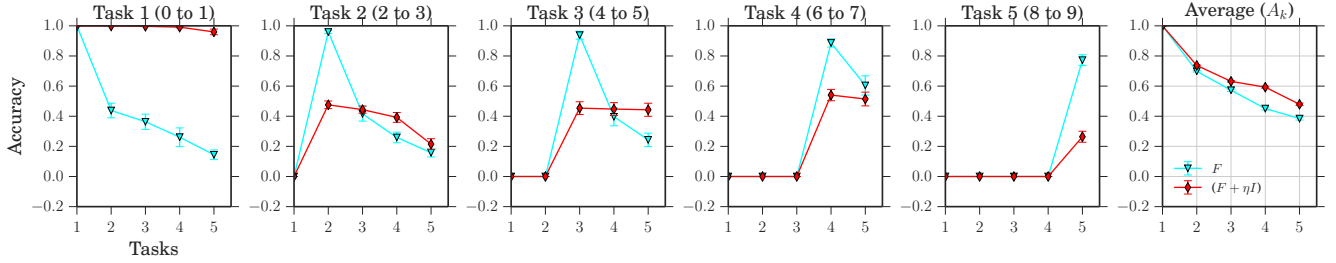


Figure 6: Accuracy measure in incremental MNIST with F and $(F + \eta I)$ used to regularize the parameters. Note that, with $(F + \eta I)$ after training for the second task the model maintains the performance on the first task, whereas with just F the performance on the first task deteriorates as the model is trained for the second task. This validates that passing a constant curvature along with the Fisher matrix avoid forgetting when a task achieves a local minimum. Note: The plots are generated with the best values of (λ, η) for our method reported in Table 3. This is why the plot with F behaves differently than the EWC one in Fig 5. (best viewed in color)

zero η passes a constant curvature at the local minimum and, hence, avoids forgetting on the first task. This behaviour is also exhibited in the Fig. 6 where we replaced the F matrix in the EWC with $(F + \eta I)$.

C.3. Effect of Increasing the Number of Samples

In Fig. 8 we compare the average accuracy and forgetting measure for different methods as the number of samples are increased. It can be seen from the plots that with increasing samples the accuracy on the regularized models plateaus whereas standard *SGD* (Vanilla) achieves consistent gains in performance. This happens because the regularized mod-

els try to keep the parameters value close to the ones they found for earlier tasks, thereby, restricting the exploration during the objective function optimization. Standard *SGD*, on the other hand, does not constraint the exploration in anyway and ends up learning better minimum for all the tasks. If we increase the number of samples further, standard *SGD* would outperform the other methods but one cannot expect to store huge number of samples from previous classes. Hence, comparison at smaller number of samples should be considered for an incremental learning setting.

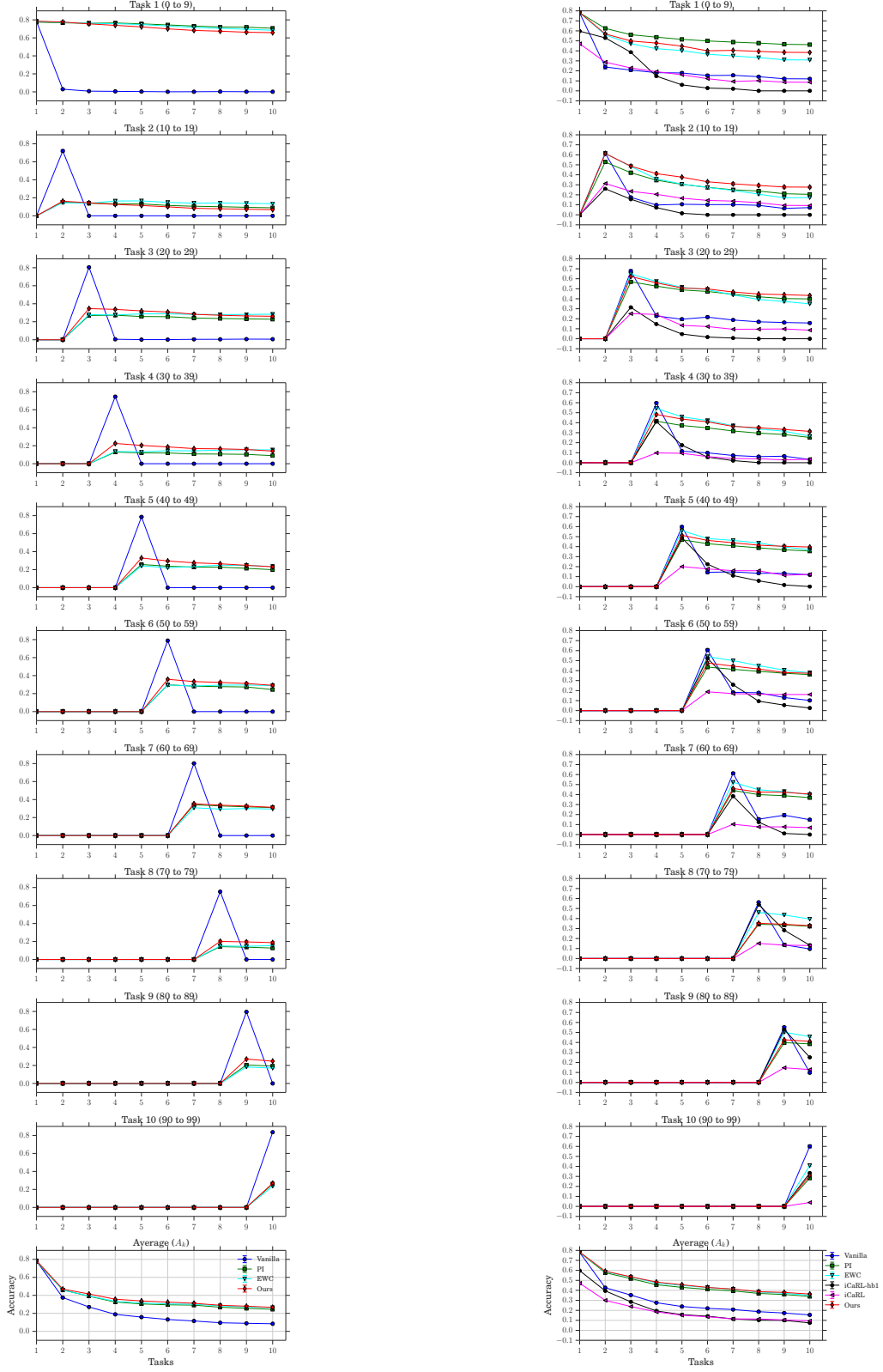


Figure 7: Accuracy measure in incremental CIFAR-100 without (*left*) and with (*right*) sampling as the model is trained for new tasks. (*best viewed in color*)

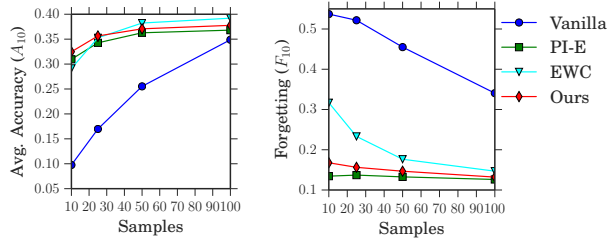


Figure 8: CIFAR-100: Comparison of different methods against the number of samples. Our method maintains comparable or better accuracy than other methods, while keeping a low forgetting measure with increasing number of samples. (best viewed in color)

References

- [1] M. Abadi, A. Agarwal, P. Barham, E. Brevdo, Z. Chen, C. Citro, G. S. Corrado, A. Davis, J. Dean, M. Devin, and others. Tensorflow: Large-scale machine learning on heterogeneous distributed systems. *arXiv preprint arXiv:1603.04467*, 2016. 6
- [2] S.-I. Amari. Natural gradient works efficiently in learning. *Neural Computation*, 1998. 2, 3, 9
- [3] R. Grosse and J. Martens. A kronecker-factored approximate fisher matrix for convolution layers. In *ICML*, pages 573–582, 2016. 4
- [4] R. Hecht-Nielsen et al. Theory of the backpropagation neural network. *Neural Networks*, 1(Supplement-1):445–448, 1988. 6
- [5] G. Hinton, O. Vinyals, and J. Dean. Distilling the knowledge in a neural network. In *NIPS*, 2014. 1, 6
- [6] D. Kingma and J. Ba. Adam: A method for stochastic optimization. *arXiv preprint arXiv:1412.6980*, 2014. 6
- [7] J. Kirkpatrick, R. Pascanu, N. C. Rabinowitz, J. Veness, G. Desjardins, A. A. Rusu, K. Milan, J. Quan, T. Ramalho, A. Grabska-Barwinska, D. Hassabis, C. Clopath, D. Kumaran, and R. Hadsell. Overcoming catastrophic forgetting in neural networks. *Proceedings of the National Academy of Sciences of the United States of America (PNAS)*, 2016. 1, 2, 3, 4, 5, 6, 11
- [8] A. Krizhevsky and G. Hinton. Learning multiple layers of features from tiny images. <https://www.cs.toronto.edu/~kriz/cifar.html>, 2009. 2
- [9] S. Kullback and R. A. Leibler. On information and sufficiency. *The Annals of Mathematical Statistics*, 1951. 2, 3
- [10] Y. LeCun. The mnist database of handwritten digits. <http://yann.lecun.com/exdb/mnist/>, 1998. 2
- [11] J. Lee, J. Yun, S. Hwang, and E. Yang. Lifelong learning with dynamically expandable networks. *arXiv preprint arXiv:1708.01547*, 2017. 6
- [12] J. M. Lee. *Riemannian manifolds: an introduction to curvature*, volume 176. Springer Science & Business Media, 2006. 3
- [13] S.-W. Lee, J.-H. Kim, J.-W. Ha, and B.-T. Zhang. Overcoming catastrophic forgetting by incremental moment matching. In *NIPS*, 2017. 6
- [14] Z. Li and D. Hoiem. Learning without forgetting. In *European Conference on Computer Vision*, pages 614–629, 2016. 2, 6
- [15] T.-Y. Lin, P. Goyal, R. Girshick, K. He, and P. Dollár. Focal loss for dense object detection. *arXiv preprint arXiv:1708.02002*, 2017. 6
- [16] D. Lopez-Paz and M. Ranzato. Gradient episodic memory for continuum learning. In *NIPS*, 2017. 2, 6
- [17] J. Martens. *Second-order optimization for neural networks*. PhD thesis, University of Toronto (Canada), 2016. 3
- [18] J. Martens and R. Grosse. Optimizing neural networks with kronecker-factored approximate curvature. In *ICML*, pages 2408–2417, 2015. 5
- [19] R. Pascanu and Y. Bengio. Revisiting natural gradient for deep networks. In *ICLR*, 2014. 2, 3, 9
- [20] S.-A. Rebuffi, H. Bilen, and A. Vedaldi. Learning multiple visual domains with residual adapters. In *NIPS*, 2017. 6
- [21] S.-V. Rebuffi, A. Kolesnikov, and C. H. Lampert. iCaRL: Incremental classifier and representation learning. In *CVPR*, 2017. 2, 5, 6, 7, 8, 9
- [22] A. A. Rusu, N. C. Rabinowitz, G. Desjardins, H. Soyer, J. Kirkpatrick, K. Kavukcuoglu, R. Pascanu, and R. Hadsell. Progressive neural networks. *arXiv preprint arXiv:1606.04671*, 2016. 6
- [23] A. V. Terekhov, G. Montone, and J. K. ORegan. Knowledge transfer in deep block-modular neural networks. In *Conference on Biomimetic and Biohybrid Systems*, pages 268–279, 2015. 6
- [24] F. Zenke, B. Poole, and S. Ganguli. Continual learning through synaptic intelligence. In *ICML*, 2017. 1, 2, 4, 6, 7, 11